iScience

CellPress
OPEN ACCESS

Article

Downregulation of VPS13C promotes cisplatin resistance in cervical cancer by upregulating GSTP1

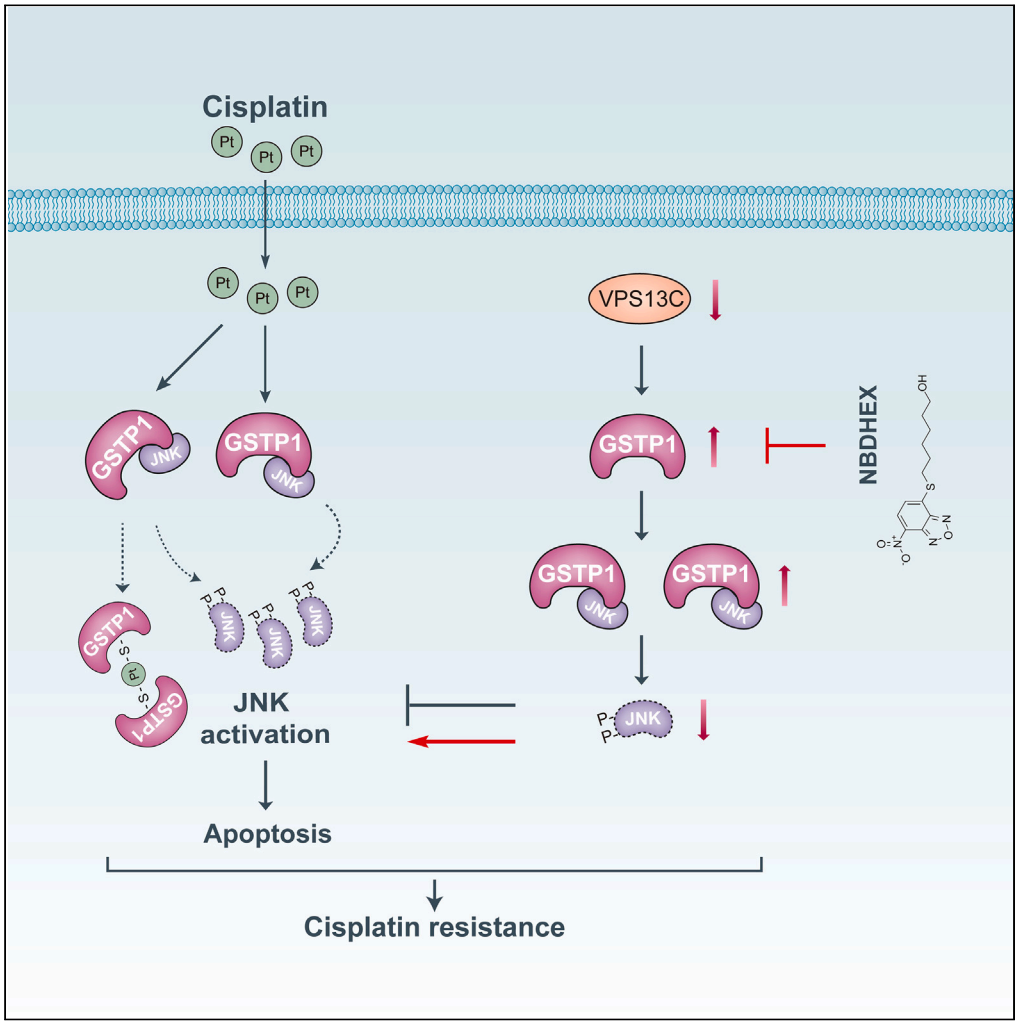

Xiangyu Tan, Xueqian Wang, Xueyao Liao, ..., Danni Gong, Zheng Hu, Xun Tian

huzheng1998@163.com (Z.H.)
tianxun@zxhospital.com (X.T.)

Highlights

Loss of VPS13C promotes cisplatin resistance in cervical cancer

VPS13C deficiency upregulates the expression of GSTP1 and inhibits the JNK pathway

Targeting GSTP1 with inhibitor NBDHEX attenuates cisplatin resistance induced by VPS13C deficiency

Tan et al., iScience 26, 107315
August 18, 2023
https://doi.org/10.1016/j.isci.2023.107315

iScience

CellPress
OPEN ACCESS

Article

Downregulation of VPS13C promotes cisplatin resistance in cervical cancer by upregulating GSTP1

Xiangyu Tan,[1,3,8] Xueqian Wang,[1,3,8] Xueyao Liao,[2] Xin Wang,[1,3] Zhichao Jiang,[2] Wenjia Liang,[2] Chen Cao,[2] Danni Gong,[2] Zheng Hu,[4,5,6,7,*] and Xun Tian[1,2,3,9,*]

SUMMARY

Cisplatin resistance remains a major obstacle limiting the effectiveness of chemotherapy in cervical cancer. However, the underlying mechanism of cisplatin resistance is still unclear. In this study, we demonstrate that vacuolar protein sorting 13 homolog C (VPS13C) deficiency promotes cisplatin resistance in cervical cancer. Moreover, through an RNA sequencing screen, VPS13C deficiency was identified as negatively correlated with the high expression of glutathione S-transferase pi gene (GSTP1). Mechanistically, loss of VPS13C contributes to cisplatin resistance by influencing the expression of GSTP1 and inhibiting the downstream c-Jun N-terminal kinase (JNK) pathway. In addition, targeting GSTP1 with the inhibitor NBDHEX effectively rescued the cisplatin resistance induced by VPS13C deficiency. Overall, our findings provide insights into the underlying mechanisms of VPS13C in cisplatin resistance and identify VPS13C as a promising candidate for the treatment of chemoresistance in cervical cancer.

INTRODUCTION

Cervical cancer is the fourth most common malignancy in women globally.[1] In 2020, there were approximately 604,000 new cases and 342,000 related deaths worldwide.[2] Currently, platinum-based chemotherapy remains the standard treatment for patients with advanced cervical cancer.[3,4] However, intrinsic or acquired cisplatin resistance severely limits the curative efficacy in patients with cervical cancer and results in chemotherapy failure.[5,6] Therefore, there is an urgent need to elucidate the mechanism of cisplatin resistance to improve the effectiveness of chemotherapy for cervical cancer. The molecular mechanism of cisplatin resistance is complex and mainly involves increased drug efflux, drug breakdown, increased DNA damage repair, and inactivation of apoptosis.[7] Unfortunately, the underlying mechanism of cisplatin resistance in cervical cancer is still unclear.

Vacuolar protein sorting 13 homolog C (VPS13C), a member of the vacuolar protein sorting-associated 13 gene family, encodes lipid transfer proteins that localize to contact sites between the endoplasmic reticulum and late endosomes/lysosomes.[8] Mutation of VPS13C plays a crucial role in autosomal-recessive early-onset Parkinson's disease and type 2 diabetes.[9,10] Many genome-wide association studies have proven that VPS13C mutation is also related to many cancers, including endometrial cancer and gastric and colorectal cancers.[11,12] We recently reported that loss of VPS13C contributes to cisplatin resistance in cervical cancer cells.[13] However, the underlying molecular mechanisms by which VPS13C contributes to cisplatin resistance in cervical cancer are still unclear.

In this study, we further demonstrated that VPS13C deficiency contributes to cisplatin resistance in cervical cancer both *in vitro* and *in vivo*. Mechanistically, VPS13C negatively influences the expression of GSTP1 and alters the downstream c-Jun N-terminal kinase (JNK) pathway. In addition, 6-(7-nitro-2,1,3-benzoxadiazol-4-ylthio) hexanol (NBDHEX), as an inhibitor of GSTP1, can reverse cisplatin resistance induced by VPS13C deficiency.

RESULTS

VPS13C deficiency promotes cisplatin resistance in cervical cancer cells

Our recent research demonstrated that loss of VPS13C confers cisplatin resistance to cervical cancer SiHa cells.[13] In this study, to further confirm the effect of VPS13C on cisplatin resistance, we selected two cervical cancer cell lines SiHa and ME180 for subsequent experiments. VPS13C-knockdown SiHa cells were

[1]Department of Obstetrics and Gynecology, Tongji Hospital, Tongji Medical College, Huazhong University of Science and Technology, Wuhan, Hubei 430030, China

[2]Department of Obstetrics and Gynecology, Academician Expert Workstation, The Central Hospital of Wuhan, Tongji Medical College, Huazhong University of Science and Technology, Wuhan, Hubei 430014, China

[3]National Clinical Research Center for Obstetrics and Gynecology, Cancer Biology Research Center (Key Laboratory of the Ministry of Education), Tongji Hospital, Tongji Medical College, Huazhong University of Science and Technology, Wuhan, Hubei 430110, China

[4]Department of Gynecologic Oncology, Zhongnan Hospital of Wuhan University, Wuhan 430071, China

[5]Department of Radiation and Medical Oncology, Zhongnan Hospital of Wuhan University, Wuhan 430071 Hubei, China

[6]Hubei Key Laboratory of Tumor Biological Behaviors, Zhongnan Hospital of Wuhan University, Wuhan 430071 Hubei, China

[7]Hubei Cancer Clinical Study Center, Zhongnan Hospital of Wuhan University, Wuhan 430071 Hubei, China

[8]These authors contributed equally

[9]Lead contact

*Correspondence: huzheng1998@163.com (Z.H.), tianxun@zxhospital.com (X.T.)

https://doi.org/10.1016/j.isci.2023.107315

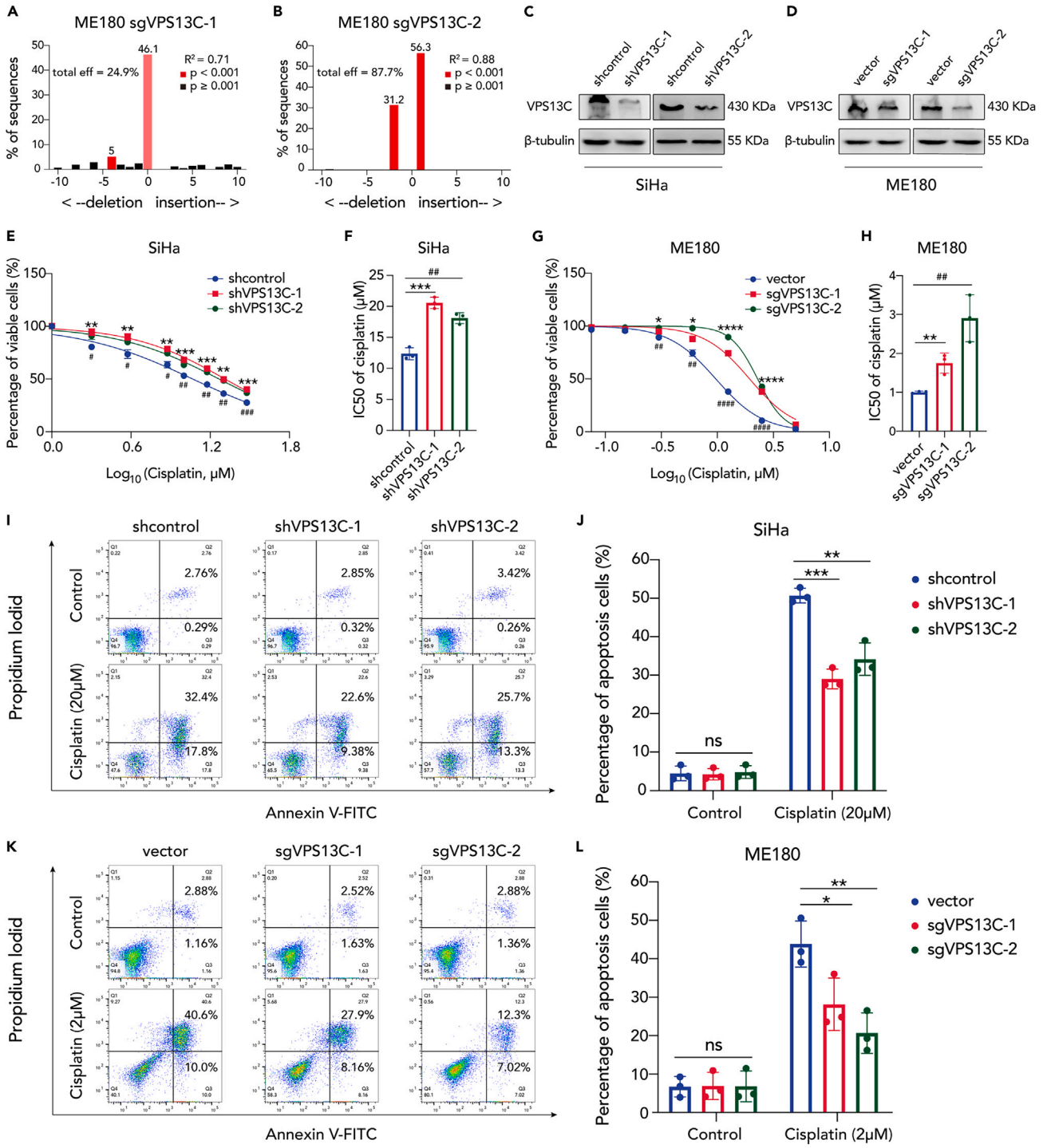

Figure 1. VPS13C deficiency promotes cisplatin resistance in cervical cancer cells

(A and B) The VPS13C mutation in ME180 cells was detected by Sanger sequencing and analyzed by the TIDE online tool.

(C and D) The protein level of VPS13C in stable SiHa and ME180 cells was analyzed by western blotting. β-Tubulin was used as the loading control.

(E and G) The viability of SiHa and ME180 cells treated with different concentrations of cisplatin was evaluated by a CCK8 assay. Data are presented as mean ± SD, n = 3.

(F and H) The half-maximal inhibitory concentration (IC50) of cisplatin in SiHa and ME180 cells was calculated and plotted with Prism software. Data represent the average of three independent experiments (mean ± SD).

Figure 1. *Continued*

(I–L) Representative flow cytometry plots (I, K) and quantification of the apoptosis rate (J, L) in SiHa and ME180 cells treated with cisplatin for 48 h. Both Annexin V+/PI- and Annexin V+/PI + cells were considered apoptotic. Data represent the average of three independent experiments (mean ± SD). For all panels, experimental significance was determined using Student's *t* test. "*" indicates a statistically significant difference between the shcontrol/vector group and the shVPS13C-1/sgVPS13C-1 group. "#" indicates a statistically significant difference between the shcontrol/vector group and the shVPS13C-2/sgVPS13C-2 group. *p < 0.05, **p < 0.01, ***p < 0.001, ****p < 0.0001, #p < 0.05, ##p < 0.01, ###p < 0.001, ####p < 0.0001, ns represents "not significant".

constructed by employing lentiviruses carrying shRNA (short hairpin RNA). VPS13C-knockout ME180 cells were generated by employing lentiviruses carrying sgRNA (single guide RNA). Three shRNAs targeting VPS13C were established in SiHa cells and the efficiency of VPS13C knockdown was measured by qPCR (Figure S1A) and western blotting (Figure 1C). Then, shRNAs with higher knockdown efficiency were selected for subsequent study. The mutation and protein expression of VPS13C in ME180 cells were detected by Sanger sequencing (Figures 1A and 1B) and western blotting (Figure 1D), respectively. In addition, we constructed stable SiHa and ME180 cells with VPS13C overexpression via CRISPR activation tools and confirmed the efficiency of overexpression by qPCR and western blotting (Figures S2A–S2D). Compared to control cells, SiHa and ME180 cells with VPS13C deficiency exhibited higher cell viability under increasing concentrations of cisplatin (Figures 1E and 1G) and a higher half-maximal inhibitory concentration (IC50) of cisplatin (Figures 1F and 1H). Similarly, lower cell viability and IC50 of cisplatin were observed in SiHa and ME180 cells with VPS13C overexpression (Figures S2E–S2H). These observations indicated that VPS13C deficiency contributes to cisplatin resistance in cervical cancer cells.

Previous studies have shown that cisplatin eradicates cancer cells by crosslinking with DNA and subsequently leading to apoptosis which is associated with cisplatin resistance.[14–16] Therefore, we next investigated the impact of VPS13C on cisplatin-induced apoptosis in cervical cancer cells. Stably transfected SiHa and ME180 cells were treated with or without 20 μM and 2 μM cisplatin for 48 h, and apoptosis was detected by flow cytometry. We found that loss of VPS13C did not alter the apoptosis rate but significantly decreased cisplatin-induced apoptosis in both SiHa and ME180 cells (Figures 1I–1L). Similarly, a higher apoptosis rate was observed in VPS13C-overexpressing SiHa and ME180 cells than in control cells under cisplatin treatment (Figures S2I–S2L). Taken together, the above results provide robust evidence that VPS13C plays an important role in cisplatin resistance in cervical cancer cells.

VPS13C expression is negatively correlated with GSTP1 expression in cervical cancer

To further explore the molecular mechanism by which VPS13C contributes to cisplatin resistance in cervical cancer, we performed gene set enrichment analysis (GSEA) by ranking genes according to their Pearson correlation with the expression of VPS13C in the TCGA dataset. Drug metabolism gene sets were significantly enriched in the group with low VPS13C expression (Figure 2A), and the top genes negatively associated with VPS13C expression and drug metabolism pathways are listed (Figure 2B). To further identify crucial pathways in VPS13C-silenced cervical cancer cells under cisplatin treatment, we performed RNA sequencing analysis on SiHa and ME180 cells treated with 20 μM and 2 μM cisplatin, respectively, for 48 h. The results showed that the differentially expressed genes between VPS13C-deficient SiHa and control cells were significantly enriched in glutathione metabolic pathways (Figure 2C), which can lead to drug resistance by enhancing the detoxification of anticancer drugs.[17,18] Consistently, the enrichment of glutathione metabolic pathways in ME180 cells was confirmed through GSEA (Figure 2D). To further narrow the predicted targets that contributed to VPS13C-induced cisplatin resistance, we generated Venn diagrams of differentially expressed genes of glutathione metabolic pathways from the TCGA dataset and RNA-seq analysis. Among these, the glutathione S-transferase pi gene (GSTP1), which was reported to play an important role in cisplatin resistance, was finally identified as a potential downstream molecule that was significantly negatively correlated with VPS13C (Figure 2E).[19,20] Subsequently, the negative correlation between VPS13C and GSTP1 mRNA levels in cervical cancer cell lines was confirmed via the LinkedOmics database (Pearson correlation = - 0.4301, p = 4.035e-15) (Figure 2F). The above results suggest that VPS13C deficiency is related to the enrichment of drug and glutathione metabolism pathways and the high expression of GSTP1.

VPS13C deficiency confers cisplatin resistance to cervical cancer by influencing GSTP1 expression and inhibiting the JNK pathway

Studies have shown that GSTP1 plays an important role in cisplatin resistance in osteosarcoma and ovarian cancer.[21,22] Therefore, we next investigated whether VPS13C deficiency confers cisplatin resistance by influencing GSTP1 expression. We first detected the mRNA expression of VPS13C and GSTP1 at the cellular level.

A

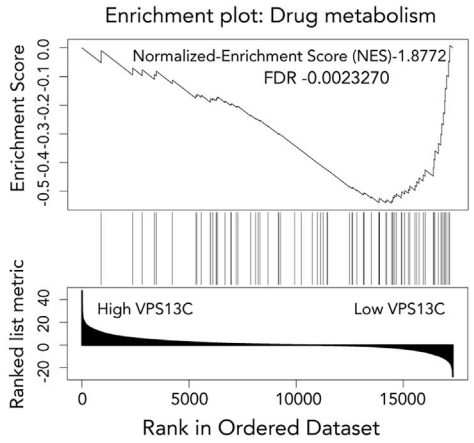

B

Gene Symbol	Entrez Gene	Score
NME2	4831	-15.257
GSTP1	2950	-14.3941
UPP1	7378	-12.8491
ITPA	3704	-12.1593
UCK2	7371	-11.8619
GSTO1	9446	-11.178
TYMP	1890	-10.5027
NME1	4830	-10.0998
NME1-NME2	654364	-9.3628
UMPS	7372	-8.4891
TK1	7083	-8.1751
UCK1	83549	-7.9144
IMPDH2	3615	-6.0217
UGT1A7	54577	-5.6931
GMPS	8833	-5.0404

C

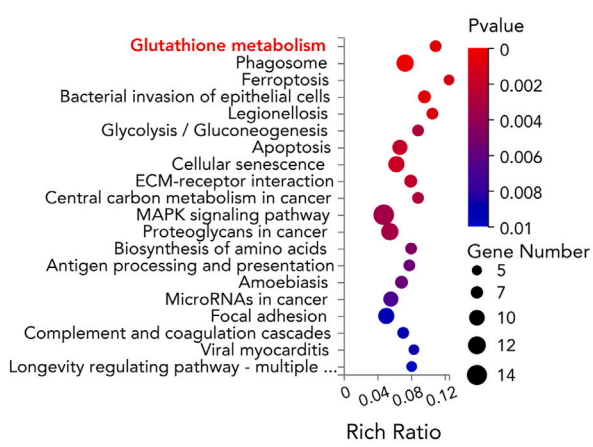

D

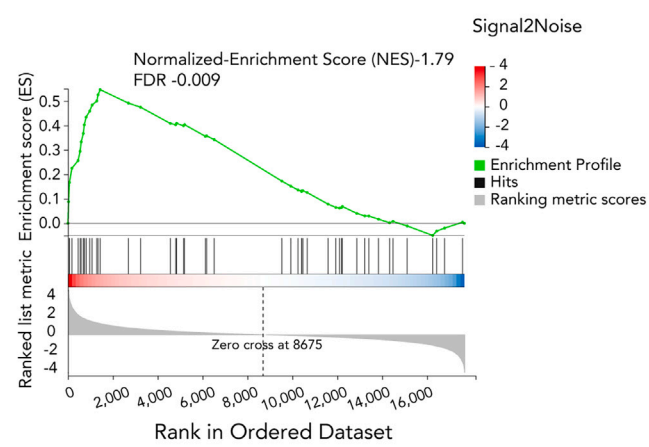

E

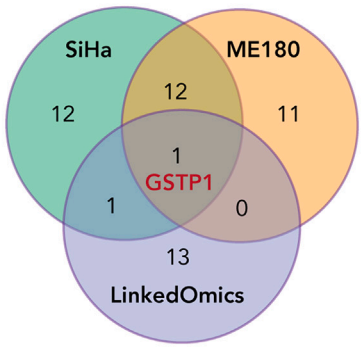

F

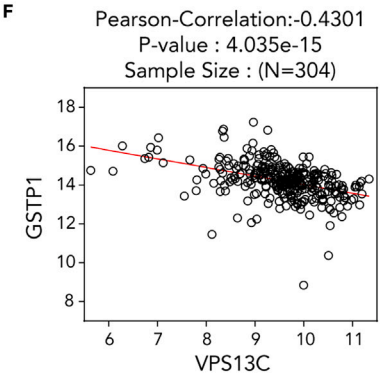

Figure 2. VPS13C expression is negatively correlated with GSTP1 expression in cervical cancer

(A) Gene set enrichment analysis based on KEGG pathways and the LinkedOmics database showed that VPS13C-related genes were significantly enriched in drug metabolism pathways.

(B) Top-ranked genes whose expression was negatively correlated with VPS13C expression in the drug metabolism pathway.

(C) KEGG pathway enrichment analysis of VPS13C-related genes in SiHa cells treated with cisplatin.

(D) GSEA plot of glutathione metabolism enrichment in ME180 cells treated with cisplatin.

(E) Venn diagram showing the overlapping genes identified by RNA-seq analysis of SiHa and ME180 cells and obtained from the LinkedOmics database.

(F) Correlation analysis of VPS13C and GSTP1 mRNA expression. Pearson's correlation coefficients and p values are shown.

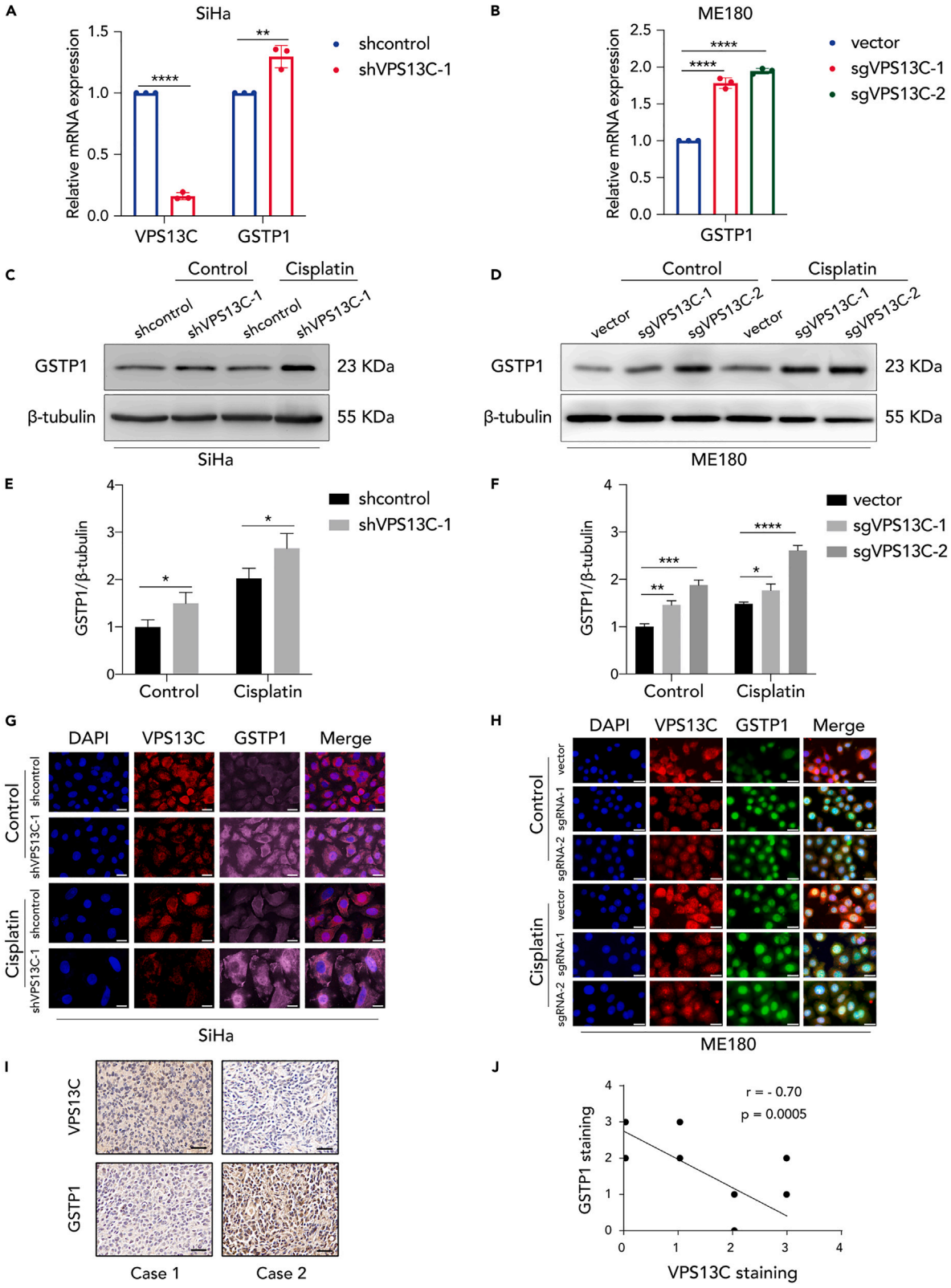
A
SiHa
Relative mRNA expression
shcontrol
shVPS13C-1
VPS13C
GSTP1
B
ME180
vector
sgVPS13C-1
sgVPS13C-2
C
Control
Cisplatin
GSTP1
β-tubulin
23 KDa
55 KDa
D
E
GSTP1/β-tubulin
F
G
DAPI
VPS13C
Merge
H
I
Case 1
Case 2
J
r = - 0.70
p = 0.0005
GSTP1 staining
VPS13C staining

Figure 3. VPS13C deficiency confers cisplatin resistance to cervical cancer by influencing GSTP1 expression

(A and B) The mRNA levels of VPS13C and GSTP1 in SiHa and ME180 cells were measured by qPCR. Data represent the average of three independent experiments (mean ± SD). Significance was determined by Student's *t* test, **p < 0.01, ****p < 0.0001.

(C and D) The protein level of GSTP1 in stable SiHa and ME180 cells was measured by western blotting.

(E and F) The relative expression of the GSTP1 protein in SiHa and ME180 cells was determined by normalization to β-tubulin. Data represent the average of three independent experiments (mean ± SD). Significance was determined by Student's *t* test, *p < 0.05, **p < 0.01, ***p < 0.001, ****p < 0.0001.

(G and H) GSTP1 and VPS13C protein expression in SiHa and ME180 cells treated with or without cisplatin for 48 h was detected by immunofluorescence staining. Nuclei were stained with DAPI. Scale bars, 20 μm.

(I) Representative immunohistochemical staining of VPS13C and VPS13C proteins in tissue slices from patients with cervical cancer. n = 20, scale bars, 30 μm.

(J) Spearman's correlation between the IHC staining scores of VPS13C and GSTP1 (p value calculated using Spearman's correlation test).

Consistent with the RNA sequencing results, both the mRNA and protein levels of GSTP1 were elevated in SiHa and ME180 cells after VPS13C knockdown (Figures 3A–3D). Similar observations were obtained through immunofluorescence staining (Figures 3G and 3H). Moreover, when VPS13C was overexpressed, the expression of GSTP1 was reduced at both mRNA and protein levels (Figures S2M–S2P). Furthermore, lower VPS13C protein expression and higher GSTP1 protein levels were observed in cisplatin-resistant SiHa/DDP cells than in parental SiHa cells (Figures S3A–S3C). The above findings encouraged us to explore the effect of VPS13C and GSTP1 on cisplatin resistance and their negative correlation in clinical samples. To further confirm the relationship between VPS13C and GSTP1, we determined their expression levels in 40 tissue specimens from 20 platinum-treated patients with cervical cancer. Immunohistochemistry analysis showed that patients with cervical cancer with cisplatin resistance had lower VPS13C and higher GSTP1 protein expression (Figure 3I). These results indicated that VPS13C expression was negatively correlated with GSTP1 expression in platinum-treated cervical cancer cases (p = 0.0005, Figure 3J). Overall, these results demonstrated that VPS13C deficiency may promote cisplatin resistance by influencing GSTP1 expression.

Given that GSTP1 plays an important role in cisplatin resistance.[23,24] Therefore, we further evaluated the effect of VPS13C deficiency on GST enzyme activity using a GST enzyme kit against substrate CDNB. The results showed that both the mRNA and protein expression of GSTP1, as well as GST enzyme activity, were increased in cervical cancer cells with VPS13C deficiency (Figures 4A and 4B). Moreover, studies have suggested that GSTP1 inhibits JNK phosphorylation by binding to JNK, which is required for downstream apoptosis signaling.[24] Subsequently, to further investigate the impact on the JNK pathway in VPS13C-deficient cell lines, we detected JNK phosphorylation by western blotting. The phosphorylation level of JNK in the VPS13C-deficient and cisplatin-resistant SiHa/DDP cells was significantly decreased compared to that in control cells (Figures 4C–4F and S3C). An increase in JNK phosphorylation level was further observed in VPS13C-overexpressing cells (Figures S2O and S2P). The above results indicated that loss of VPS13C confers cisplatin resistance to cervical cancer cells by influencing GSTP1 expression and inhibiting its downstream JNK pathway.

The GSTP1 inhibitor NBDHEX rescued the cisplatin resistance induced by VPS13C deficiency

The previously described results provide evidence that VPS13C affects the efficacy of cisplatin in cervical cancer by influencing GSTP1 expression. Therefore, we hypothesized that targeting GSTP1 may represent a potential strategy for the reversal of cisplatin resistance caused by VPS13C deficiency. NBDHEX, a specific inhibitor of GSTP1, inhibits GSTP1 by reducing GSTP1 enzyme activity and disrupting the interaction between GSTP1 and key signaling factors.[25] We first examined the effect of NBDHEX on GST enzyme activity with a GST enzyme kit, and the results showed that NBDHEX can successfully reduce the enzyme activity of cervical cancer cells, especially in cells with VPS13C knockdown (Figures 5A and 5B). Next, we conducted a CCK-8 assay to determine the effect of NBDHEX on the cell viability of cervical cancer cells. As shown in Figures 5C–5F, NBDHEX reversed the increase in cell viability induced by VPS13C deficiency under cisplatin treatment. In addition, cisplatin and NBDHEX had a synergistic effect on the inhibition of cell viability in SiHa and ME180 cells (Figures S4A–S4D). Subsequently, we further verified the effect of NBDHEX on cisplatin-induced apoptosis by flow cytometry. The results showed that NBDHEX could reverse the decrease in cisplatin-induced apoptosis in cervical cancer cells with VPS13C deficiency (Figures 5G–5J). These observations suggest that inhibition of GSTP1 could effectively attenuate the cisplatin resistance of cervical cancer cells induced by VPS13C deficiency.

The GSTP1 inhibitor NBDHEX rescued the cisplatin resistance induced by VPS13C deficiency *in vivo*

To investigate the effect of VPS13C on cisplatin resistance in cervical cancer *in vivo*, we established mouse subcutaneous xenograft models using stably transfected SiHa cells. Mice bearing subcutaneous xenografts of SiHa control and VPS13C-deficient cells were treated with cisplatin and the inhibitor NBDHEX (Figure 6A). We

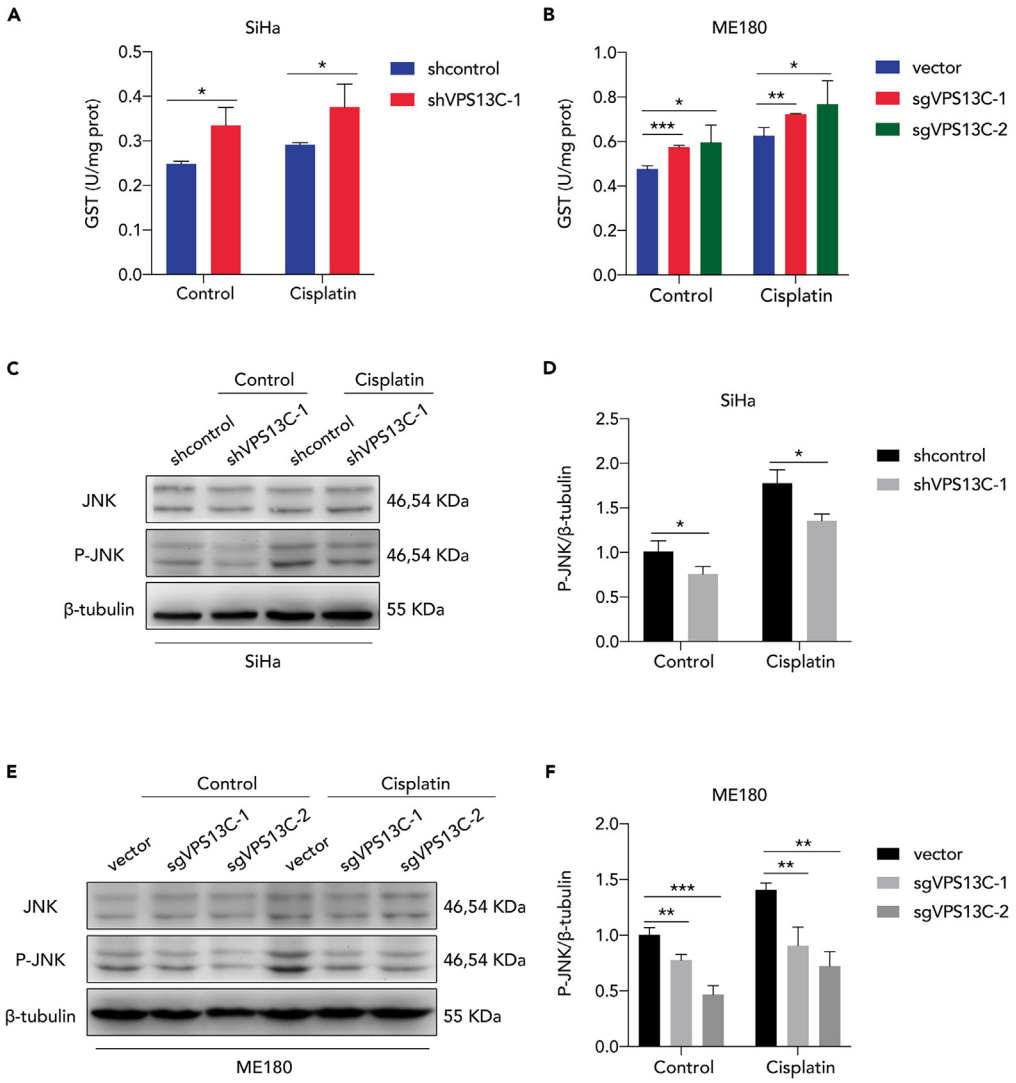

Figure 4. VPS13C deficiency increases the enzyme activity of GST and inhibits the JNK pathway

(A and B) GST enzyme activity in SiHa and ME180 cells was evaluated after exposure to cisplatin for 48 h. Data represent the average of three independent experiments (mean ± SD). Significance was determined by Student's *t* test, *p < 0.05, ***p < 0.001. (C and E) The protein levels of total and phosphorylated JNK in SiHa and ME180 cells were determined by western blotting. (D and F) The relative phosphorylation level of JNK was determined by normalization to β-tubulin. Data represent the average of three independent experiments (mean ± SD). Significance was determined by Student's *t* test, *p < 0.05, **p < 0.01, ***p < 0.001.

observed that VPS13C deficiency significantly promoted tumor growth when mice were treated with 2 or 5 mg/kg cisplatin, and NBDHEX reversed the effect of VPS13C knockdown on tumor growth (Figures 6B–6E). In addition, all treatments were well tolerated, with no significant weight loss or major clinical signs of toxicity or distress (Figures S5A and S5B). Via western blotting of the subcutaneous tumor, we demonstrated that VPS13C is negatively associated with the expression of GSTP1 (Figure 6F). Altogether, these data indicate that the GSTP1 inhibitor NBDHEX could effectively reverse cisplatin resistance induced by VPS13C deficiency in cervical cancer cells.

DISCUSSION

The 5-year survival rate of patients with cervical cancer has significantly improved over the past 30 years, but drug resistance remains a major challenge affecting prognosis.[26,27] Therefore, exploring the underlying mechanism is of great significance to improve the survival of patients with cervical cancer.

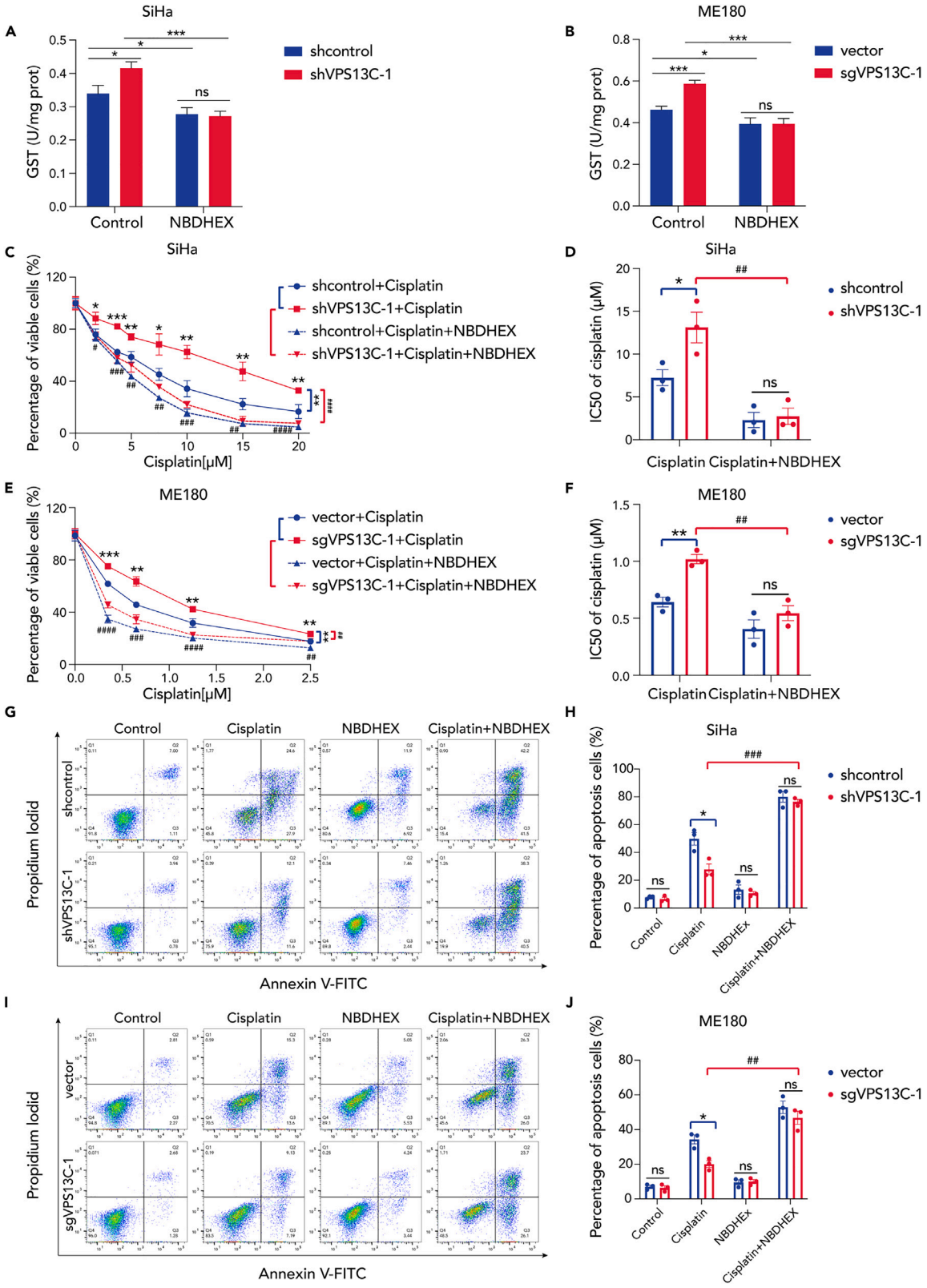
A
SiHa
GST (U/mg prot)
shcontrol
shVPS13C-1
Control
NBDHEX
B
ME180
vector
sgVPS13C-1
C
SiHa
Percentage of viable cells (%)
shcontrol+Cisplatin
shVPS13C-1+Cisplatin
shcontrol+Cisplatin+NBDHEX
shVPS13C-1+Cisplatin+NBDHEX
Cisplatin[μM]
D
SiHa
IC50 of cisplatin (μM)
Cisplatin
Cisplatin+NBDHEX
E
ME180
vector+Cisplatin
sgVPS13C-1+Cisplatin
vector+Cisplatin+NBDHEX
sgVPS13C-1+Cisplatin+NBDHEX
F
ME180
G
Control
Cisplatin
NBDHEX
Cisplatin+NBDHEX
Propidium Iodid
shcontrol
shVPS13C-1
Annexin V-FITC
H
SiHa
Percentage of apoptosis cells (%)
I
vector
sgVPS13C-1
J
ME180

Figure 5. The GSTP1 inhibitor NBDHEX rescued cisplatin resistance induced by VPS13C deficiency

(A and B) The catalytic activity of GST in SiHa and ME180 cells treated with or without the GSTP1 inhibitor NBDHEX. Data represent the average of three independent experiments (mean ± SD).

(C and E) The viability of stable SiHa and ME180 cells treated with increasing concentrations of cisplatin and a fixed concentration of NBDHEX for 48 h was evaluated by a CCK-8 assay. Data are presented as mean ± SD, n = 3.

(D and F) The IC50 value of cisplatin in SiHa and ME180 cells was calculated and plotted with GraphPad Prism. Data represent the average of three independent experiments (mean ± SD).

(G–J) Representative flow cytometry plots (G, I) and quantification of the apoptosis rate (H, J) in SiHa and ME180 cells treated with cisplatin and NBDHEX for 48 h. Both Annexin V+/PI- and Annexin V+/PI + cells were considered apoptotic. Data represent the average of three independent experiments (mean ± SD). For all panels, experimental significance was determined using Student's *t* test. "*" represents comparisons between the control/vector+cisplatin and shVPS13C/sgVPS13C + cisplatin groups. "#" represents comparisons between the shVPS13C/sgVPS13C + cisplatin and shVPS13C/sgVPS13C+cisplatin +NBDHEX groups. *p < 0.05, **p < 0.01, ***p < 0.001, ****p < 0.0001, #p < 0.05, ##p < 0.01, ###p < 0.001, ####p < 0.0001, ns represents "not significant".

In recent years, research on VPS13C has mainly focused on Parkinson's and metabolic diseases.[28–30] However, its role in cervical cancer and cisplatin resistance remains unclear. In this study, we demonstrated that loss of VPS13C promotes cisplatin resistance in cervical cancer cells *in vitro* and *in vivo* by influencing GSTP1 expression. Studies have shown that VPS13C localizes at endosomes/lysosomes (LE/Lys), endoplasmic reticulum (ER), and lipid droplets.[8,31] VPS13C mediates lipid transfer between LE/Lys and ER and participates in lysosome homeostasis and mitochondrial dysfunction.[32–34] On the other hand, the phase II detoxifying enzyme GSTP1 is reported to play an important role in maintaining homeostasis of ER and mitochondria protection against oxidative stress.[35–37] In the present study, when VPS13C was knocked down, GSTP1 increased at the mRNA and protein levels. We speculate that increased expression of GSTP1 may be a response to the perturbation of homeostasis in LE/Lys, ER, or mitochondria, which is induced by VPS13C depletion. However, further exploration is still needed to fully elucidate the molecular mechanisms by which VPS13C influences GSTP1 in subsequent research.

Studies have shown that GSTP1 may affect cisplatin resistance through detoxifying cisplatin by isolating and inactivating cisplatin and inhibiting the downstream JNK pathway.[24,38,39] Our data suggested that the downregulation of VPS13C in cervical cancer cells leads to high mRNA and protein expression of GSTP1 and inhibition of the JNK apoptosis pathway, resulting in cisplatin resistance. In addition, we further demonstrated that the GSTP1 inhibitor NBDHEX could reverse cisplatin resistance caused by VPS13C deficiency *in vitro* and *in vivo*. From a clinical perspective, our findings provide a promising therapeutic strategy by which targeting GSTP1 can overcome cisplatin resistance in cervical cancer caused by VPS13C deficiency.

Many studies have shown that cisplatin resistance remains an important obstacle to prognosis for many solid tumors,[40–42] which encourages us to further explore the role of VPS13C in cisplatin resistance in other solid tumors. Through GDSC database analysis, we found that low VPS13C mRNA expression was associated with a higher IC50 value of cisplatin and shorter overall survival (Figures S6A–S6C). Subsequently, we further investigated the mechanism by which VPS13C deficiency promotes cisplatin resistance in these tumors based on the LinkedOmics database. Consistent with the results in cervical cancer, the drug metabolism pathway was significantly enriched in tumors with low VPS13C expression (Figure S6D), and the mRNA expression of VPS13C was negatively associated with GSTP1 in these tumors (Figure S6E). The previously described results further indicate that VPS13C deficiency may also contribute to cisplatin resistance in lung, breast, and gastric cancers. Collectively, our findings provide evidence for further exploring the versatile role of VPS13C in the chemoresistance of many solid tumors. We hope to further investigate in subsequent research to advance our understanding of the effect of VPS13C on chemoresistance.

In summary, we found that loss of VPS13C promotes cisplatin resistance in cervical cancer by influencing GSTP1 expression and inhibiting the JNK apoptosis pathway. Targeting GSTP1 with the inhibitor NBDHEX can overcome the cisplatin resistance induced by VPS13C deficiency. Moreover, VPS13C plays an important role in cisplatin resistance in other solid tumors. Taken together, our findings highlight the important role of VPS13C in cisplatin resistance and provide a potential strategy for the precision treatment of patients with cervical cancer.

Limitations of the study

Our data suggested that VPS13C deficiency promotes cisplatin resistance by influencing the expression of GSTP1. However, future functional studies will be required to elucidate the molecular mechanisms by which

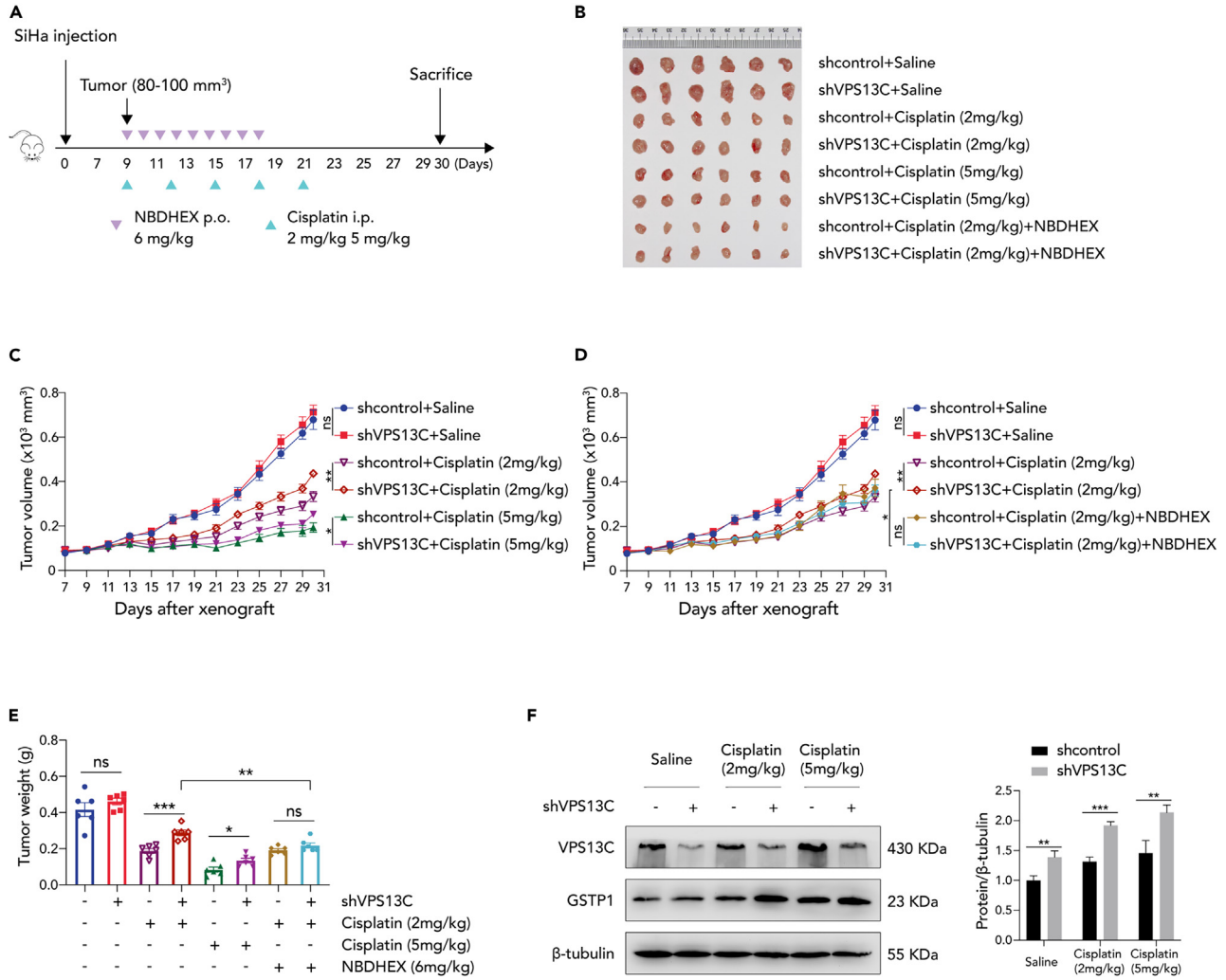

Figure 6. The GSTP1 inhibitor NBDHEX rescued cisplatin resistance induced by VPS13C deficiency *in vivo*

(A) Schematic diagram of the establishment of SiHa xenograft mice treated with cisplatin and NBDHEX *in vivo*.

(B) Images of tumors from SiHa xenograft mice.

(C and D) The inhibitory effect of different treatments on tumor volume. Data are shown as the mean ± SEM, n = 6. Significance was determined using Student's *t* test. *p < 0.05, **p < 0.01, ns represents "not significant".

(E) The weight of subcutaneously transplanted tumors in different treatment groups. Data are shown as the mean ± SEM, n = 6. Significance was determined using Student's *t* test. *p < 0.05, **p < 0.01, ***p < 0.001, ns represents "not significant".

(F) VPS13C and GSTP1 protein expression in xenograft mice. Relative protein expression of GSTP1 was determined by normalization to β-tubulin. Data represent the average of three independent experiments (mean ± SD). **p < 0.01, ***p < 0.001.

VPS13C influences GSTP1 expression. In addition, bioinformatics analysis suggested that VPS13C is also involved in cisplatin resistance in other solid tumors, which needs to be confirmed by experiments in the future. Despite these limitations, our data revealed an important role of VPS13C in cisplatin resistance of cervical cancer.

STAR★METHODS

Detailed methods are provided in the online version of this paper and include the following:

- KEY RESOURCES TABLE
- RESOURCE AVAILABILITY
  - Lead contact
  - Materials availability

SUPPLEMENTAL INFORMATION

Supplemental information can be found online at https://doi.org/10.1016/j.isci.2023.107315.

ACKNOWLEDGMENTS

This work was supported by the National Natural Science Foundation of China (82172584, 81902663), the Medical Research Project of Wuhan Municipal Health Commission (WX21Q09), the Natural Science Foundation of Hubei Province (2022CFB133), and the Young Top-notch Talent Cultivation Program of Hubei Public Health.

AUTHOR CONTRIBUTIONS

X.Y.T. conducted the experiments, created the figures, and wrote the manuscript; X.Y.L., X.Q.W. and Z.C.J. carried out the experimental work and data analysis; X.W., W.J.L., D.N.G., and C.C. analyzed data and performed the statistical analysis. X.T. and Z.H. designed the study and revised the manuscript.

DECLARATION OF INTERESTS

The authors declare no competing interests.

INCLUSION AND DIVERSITY

We support inclusive, diverse, and equitable conduct of research.

Received: October 7, 2022
Revised: March 5, 2023
Accepted: July 4, 2023
Published: July 10, 2023

REFERENCES

1. Bray, F., Ferlay, J., Soerjomataram, I., Siegel, R.L., Torre, L.A., and Jemal, A. (2018). Global cancer statistics 2018: GLOBOCAN estimates of incidence and mortality worldwide for 36 cancers in 185 countries. CA. Cancer J. Clin. *68*, 394–424. https://doi.org/10.3322/caac.21492.

2. Sung, H., Ferlay, J., Siegel, R.L., Laversanne, M., Soerjomataram, I., Jemal, A., and Bray, F. (2021). Global Cancer Statistics 2020: GLOBOCAN Estimates of Incidence and Mortality Worldwide for 36 Cancers in 185 Countries. CA. Cancer J. Clin. *71*, 209–249. https://doi.org/10.3322/caac.21660.

3. NCCN Clinical Practice Guidelines in Oncology (NCCN Guidelines) cervical cancer (2022). National Comprehensive Cancer Network Version 1.2022 - October 26, 2021.

4. Tangjitgamol, S., Katanyoo, K., Laopaiboon, M., Lumbiganon, P., Manusirivithaya, S., and Supawattanabodee, B. (2014). Adjuvant chemotherapy after concurrent

chemoradiation for locally advanced cervical cancer. Cochrane Database Syst. Rev. *2014*, CD010401. https://doi.org/10.1002/14651858.CD010401.pub2.

5. Ghosh, S. (2019). Cisplatin: The first metal based anticancer drug. Bioorg. Chem. *88*, 102925. https://doi.org/10.1016/j.bioorg.2019.102925.

6. Lorusso, D., Petrelli, F., Coinu, A., Raspagliesi, F., and Barni, S. (2014). A systematic review comparing cisplatin and carboplatin plus paclitaxel-based chemotherapy for recurrent or metastatic cervical cancer. Gynecol. Oncol. *133*, 117–123. https://doi.org/10.1016/j.ygyno.2014.01.042.

7. Zhu, H., Luo, H., Zhang, W., Shen, Z., Hu, X., and Zhu, X. (2016). Molecular mechanisms of cisplatin resistance in cervical cancer. Drug Des. Dev. Ther. *10*, 1885–1895. https://doi.org/10.2147/DDDT.S106412.

8. Kumar, N., Leonzino, M., Hancock-Cerutti, W., Horenkamp, F.A., Li, P., Lees, J.A., Wheeler, H., Reinisch, K.M., and De Camilli, P. (2018). VPS13A and VPS13C are lipid transport proteins differentially localized at ER contact sites. J. Cell Biol. *217*, 3625–3639. https://doi.org/10.1083/jcb.201807019.

9. Mehta, Z.B., Fine, N., Pullen, T.J., Cane, M.C., Hu, M., Chabosseau, P., Meur, G., Velayos-Baeza, A., Monaco, A.P., Marselli, L., et al. (2016). Changes in the expression of the type 2 diabetes-associated gene VPS13C in the beta-cell are associated with glucose intolerance in humans and mice. Am. J. Physiol. Endocrinol. Metab. *311*, E488–E507. https://doi.org/10.1152/ajpendo.00074.2016.

10. Foo, J.N., Tan, L.C., Irwan, I.D., Au, W.L., Low, H.Q., Prakash, K.M., Ahmad-Annuar, A., Bei, J., Chan, A.Y., Chen, C.M., et al. (2017). Genome-wide association study of Parkinson's disease in East Asians. Hum. Mol. Genet. *26*, 226–232. https://doi.org/10.1093/hmg/ddw379.

11. Chang, Y.S., Huang, H.D., Yeh, K.T., and Chang, J.G. (2017). Identification of novel mutations in endometrial cancer patients by whole-exome sequencing. Int. J. Oncol. *50*, 1778–1784. https://doi.org/10.3892/ijo.2017.3919.

12. An, C.H., Kim, Y.R., Kim, H.S., Kim, S.S., Yoo, N.J., and Lee, S.H. (2012). Frameshift mutations of vacuolar protein sorting genes in gastric and colorectal cancers with microsatellite instability. Hum. Pathol. *43*, 40–47. https://doi.org/10.1016/j.humpath.2010.03.015.

13. Tian, X., Wang, X., Cui, Z., Liu, J., Huang, X., Shi, C., Zhang, M., Liu, T., Du, X., Li, R., et al. (2021). A Fifteen-Gene Classifier to Predict Neoadjuvant Chemotherapy Responses in Patients with Stage IB to IIB Squamous Cervical Cancer. Adv. Sci. *8*, 2001978. https://doi.org/10.1002/advs.202001978.

14. Siddik, Z.H. (2003). Cisplatin: mode of cytotoxic action and molecular basis of resistance. Oncogene *22*, 7265–7279. https://doi.org/10.1038/sj.onc.1206933.

15. Pabla, N., Huang, S., Mi, Q.S., Daniel, R., and Dong, Z. (2008). ATR-Chk2 signaling in p53 activation and DNA damage response during cisplatin-induced apoptosis. J. Biol. Chem. *283*, 6572–6583. https://doi.org/10.1074/jbc.M707568200.

16. Galluzzi, L., Senovilla, L., Vitale, I., Michels, J., Martins, I., Kepp, O., Castedo, M., and Kroemer, G. (2012). Molecular mechanisms of cisplatin resistance. Oncogene *31*, 1869–1883. https://doi.org/10.1038/onc.2011.384.

17. Bansal, A., and Simon, M.C. (2018). Glutathione metabolism in cancer progression and treatment resistance. J. Cell Biol. *217*, 2291–2298. https://doi.org/10.1083/jcb.201804161.

18. Amable, L. (2016). Cisplatin resistance and opportunities for precision medicine. Pharmacol. Res. *106*, 27–36. https://doi.org/10.1016/j.phrs.2016.01.001.

19. Cui, J., Li, G., Yin, J., Li, L., Tan, Y., Wei, H., Liu, B., Deng, L., Tang, J., Chen, Y., and Yi, L. (2020). GSTP1 and cancer: Expression, methylation, polymorphisms and signaling (Review). Int. J. Oncol. *56*, 867–878. https://doi.org/10.3892/ijo.2020.4979.

20. Dong, S.C., Sha, H.H., Xu, X.Y., Hu, T.M., Lou, R., Li, H., Wu, J.Z., Dan, C., and Feng, J. (2018). Glutathione S-transferase pi: a potential role in antitumor therapy. Drug Des. Dev. Ther. *12*, 3535–3547. https://doi.org/10.2147/DDDT.S169833.

21. Pasello, M., Michelacci, F., Scionti, I., Hattinger, C.M., Zuntini, M., Caccuri, A.M., Scotlandi, K., Picci, P., and Serra, M. (2008). Overcoming glutathione S-transferase P1-related cisplatin resistance in osteosarcoma. Cancer Res. *68*, 6661–6668. https://doi.org/10.1158/0008-5472.CAN-07-5840.

22. Sawers, L., Ferguson, M.J., Ihrig, B.R., Young, H.C., Chakravarty, P., Wolf, C.R., and Smith, G. (2014). Glutathione S-transferase P1 (GSTP1) directly influences platinum drug chemosensitivity in ovarian tumour cell lines. Br. J. Cancer *111*, 1150–1158. https://doi.org/10.1038/bjc.2014.386.

23. Wang, T., Arifoglu, P., Ronai, Z., and Tew, K.D. (2001). Glutathione S-transferase P1-1 (GSTP1-1) inhibits c-Jun N-terminal kinase (JNK1) signaling through interaction with the C terminus. J. Biol. Chem. *276*, 20999–21003. https://doi.org/10.1074/jbc.M101355200.

24. De Luca, A., Parker, L.J., Ang, W.H., Rodolfo, C., Gabbarini, V., Hancock, N.C., Palone, F., Mazzetti, A.P., Menin, L., Morton, C.J., et al. (2019). A structure-based mechanism of cisplatin resistance mediated by glutathione transferase P1-1. Proc. Natl. Acad. Sci. USA *116*, 13943–13951. https://doi.org/10.1073/pnas.1903297116.

25. Federici, L., Lo Sterzo, C., Pezzola, S., Di Matteo, A., Scaloni, F., Federici, G., and Caccuri, A.M. (2009). Structural basis for the binding of the anticancer compound 6-(7-nitro-2,1,3-benzoxadiazol-4-ylthio)hexanol to human glutathione s-transferases. Cancer Res. *69*, 8025–8034. https://doi.org/10.1158/0008-5472.CAN-09-1314.

26. Bacorro, W., Baldivia, K., Yu, K.K., Mariano, J., Gonzalez, G., and Sy Ortin, T. (2022). Outcomes with definitive radiotherapy among patients with locally advanced cervical cancer with relative or absolute contraindications to cisplatin: A systematic review and meta-analysis. Gynecol. Oncol. *166*, 614–630. https://doi.org/10.1016/j.ygyno.2022.06.018.

27. Zhou, Y., Rassy, E., Coutte, A., Achkar, S., Espenel, S., Genestie, C., Pautier, P., Morice, P., Gouy, S., and Chargari, C. (2022). Current Standards in the Management of Early and Locally Advanced Cervical Cancer: Update on the Benefit of Neoadjuvant/Adjuvant Strategies. Cancers *14*, 2449. https://doi.org/10.3390/cancers14102449.

28. Hook, S.C., Chadt, A., Heesom, K.J., Kishida, S., Al-Hasani, H., Tavaré, J.M., and Thomas, E.C. (2020). TBC1D1 interacting proteins, VPS13A and VPS13C, regulate GLUT4 homeostasis in C2C12 myotubes. Sci. Rep. *10*, 17953. https://doi.org/10.1038/s41598-020-74661-1.

29. Smolders, S., Philtjens, S., Crosiers, D., Sieben, A., Hens, E., Heeman, B., Van Mossevelde, S., Pals, P., Asselbergh, B., Dos Santos Dias, R., et al. (2021). Contribution of rare homozygous and compound heterozygous VPS13C missense mutations to dementia with Lewy bodies and Parkinson's disease. Acta Neuropathol. Commun. *9*, 25. https://doi.org/10.1186/s40478-021-01121-w.

30. Olsen, A.L., and Feany, M.B. (2021). Parkinson's disease risk genes act in glia to control neuronal alpha-synuclein toxicity. Neurobiol. Dis. *159*, 105482. https://doi.org/10.1016/j.nbd.2021.105482.

31. Dziurdzik, S.K., and Conibear, E. (2021). The Vps13 Family of Lipid Transporters and Its Role at Membrane Contact Sites. Int. J. Mol. Sci. *22*, 2905. https://doi.org/10.3390/ijms22062905.

32. Bean, B.D.M., Dziurdzik, S.K., Kolehmainen, K.L., Fowler, C.M.S., Kwong, W.K., Grad, L.I., Davey, M., Schluter, C., and Conibear, E. (2018). VPS13: A lipid transfer protein making contacts at multiple cellular locations. J. Cell Biol. *217*, 3593–3607. https://doi.org/10.1083/jcb.201804111.

33. Hancock-Cerutti, W., Wu, Z., Tharkeshwar, A., Ferguson, S.M., Shadel, G.S., and De Camilli, P. (2021). ER-lysosome lipid transfer protein VPS13C/PARK23 prevents aberrant mtDNA-dependent STING signaling. Preprint at bioRxiv. https://doi.org/10.1101/2021.06.08.447593.

34. Lesage, S., Drouet, V., Majounie, E., Deramecourt, V., Jacoupy, M., Nicolas, A., Cormier-Dequaire, F., Hassoun, S.M., Pujol, C., Ciura, S., et al. (2016). Loss of VPS13C Function in Autosomal-Recessive Parkinsonism Causes Mitochondrial Dysfunction and Increases PINK1/Parkin-Dependent Mitophagy. Am. J. Hum. Genet. *98*, 500–513. https://doi.org/10.1016/j.ajhg.2016.01.014.

35. Zhang, L., Kim, S.H., Park, K.H., Zhi-Wei, Y., Jie, Z., Townsend, D.M., and Tew, K.D. (2021).

Glutathione S-Transferase P Influences Redox Homeostasis and Response to Drugs that Induce the Unfolded Protein Response in Zebrafish. J. Pharmacol. Exp. Therapeut. *377*, 121–132. https://doi.org/10.1124/jpet.120.000417.

36. Ye, Z.W., Zhang, J., Ancrum, T., Manevich, Y., Townsend, D.M., and Tew, K.D. (2017). Glutathione S-Transferase P-Mediated Protein S-Glutathionylation of Resident Endoplasmic Reticulum Proteins Influences Sensitivity to Drug-Induced Unfolded Protein Response. Antioxidants Redox Signal. *26*, 247–261. https://doi.org/10.1089/ars.2015.6486.

37. Goto, S., Kawakatsu, M., Izumi, S.I., Urata, Y., Kageyama, K., Ihara, Y., Koji, T., and Kondo, T. (2009). Glutathione S-transferase pi localizes in mitochondria and protects against oxidative stress. Free Radic. Biol. Med. *46*, 1392–1403. https://doi.org/10.1016/j.freeradbiomed.2009.02.025.

38. Chen, J., Solomides, C., and Simpkins, H. (2014). Sensitization of mesothelioma cells to platinum-based chemotherapy by GSTpi knockdown. Biochem. Biophys. Res. Commun. *447*, 77–82. https://doi.org/10.1016/j.bbrc.2014.03.100.

39. Sau, A., Filomeni, G., Pezzola, S., D'Aguanno, S., Tregno, F.P., Urbani, A., Serra, M., Pasello, M., Picci, P., Federici, G., and Caccuri, A.M. (2012). Targeting GSTP1-1 induces JNK activation and leads to apoptosis in cisplatin-sensitive and -resistant human osteosarcoma cell lines. Mol. Biosyst. *8*, 994–1006. https://doi.org/10.1039/c1mb05295k.

40. Wang, W., Zhao, M., Cui, L., Ren, Y., Zhang, J., Chen, J., Jia, L., Zhang, J., Yang, J., Chen, G., et al. (2020). Characterization of a novel HDAC/RXR/HtrA1 signaling axis as a novel target to overcome cisplatin resistance in human non-small cell lung cancer. Mol. Cancer *19*, 134. https://doi.org/10.1186/s12943-020-01256-9.

41. Wang, J., Liu, R., Mo, H., Xiao, X., Xu, Q., and Zhao, W. (2021). Deubiquitinase PSMD7 promotes the proliferation, invasion, and cisplatin resistance of gastric cancer cells by stabilizing RAD23B. Int. J. Biol. Sci. *17*, 3331–3342. https://doi.org/10.7150/ijbs.61128.

42. Luo, J., Yao, J.F., Deng, X.F., Zheng, X.D., Jia, M., Wang, Y.Q., Huang, Y., and Zhu, J.H. (2018). 14, 15-EET induces breast cancer cell EMT and cisplatin resistance by up-regulating integrin alphavbeta3 and activating FAK/PI3K/AKT signaling. J. Exp. Clin. Cancer Res. *37*, 23. https://doi.org/10.1186/s13046-018-0694-6.

43. Konermann, S., Brigham, M.D., Trevino, A.E., Joung, J., Abudayyeh, O.O., Barcena, C., Hsu, P.D., Habib, N., Gootenberg, J.S., Nishimasu, H., et al. (2015). Genome-scale transcriptional activation by an engineered CRISPR-Cas9 complex. Nature *517*, 583–588. https://doi.org/10.1038/nature14136.

44. Joung, J., Konermann, S., Gootenberg, J.S., Abudayyeh, O.O., Platt, R.J., Brigham, M.D., Sanjana, N.E., and Zhang, F. (2017). Genome-scale CRISPR-Cas9 knockout and transcriptional activation screening. Nat. Protoc. *12*, 828–863. https://doi.org/10.1038/nprot.2017.016.

45. Brinkman, E.K., Chen, T., Amendola, M., and van Steensel, B. (2014). Easy quantitative assessment of genome editing by sequence trace decomposition. Nucleic Acids Res. *42*, e168. https://doi.org/10.1093/nar/gku936.

46. Chou, T.C. (2010). Drug combination studies and their synergy quantification using the Chou-Talalay method. Cancer Res. *70*, 440–446. https://doi.org/10.1158/0008-5472.CAN-09-1947.

47. Gyorffy, B., Lánczky, A., and Szállási, Z. (2012). Implementing an online tool for genome-wide validation of survival-associated biomarkers in ovarian-cancer using microarray data from 1287 patients. Endocr. Relat. Cancer *19*, 197–208. https://doi.org/10.1530/ERC-11-0329.

48. Vasaikar, S.V., Straub, P., Wang, J., and Zhang, B. (2018). LinkedOmics: analyzing multi-omics data within and across 32 cancer types. Nucleic Acids Res. *46*, D956–D963. https://doi.org/10.1093/nar/gkx1090.

49. Yang, W., Soares, J., Greninger, P., Edelman, E.J., Lightfoot, H., Forbes, S., Bindal, N., Beare, D., Smith, J.A., Thompson, I.R., et al. (2013). Genomics of Drug Sensitivity in Cancer (GDSC): a resource for therapeutic biomarker discovery in cancer cells. Nucleic Acids Res. *41*, D955–D961. https://doi.org/10.1093/nar/gks1111.

STAR★METHODS

KEY RESOURCES TABLE

REAGENT or RESOURCE	SOURCE	IDENTIFIER
Antibodies		
Anti-VPS13C pAb	Proteintech	Cat#28676-1-AP; RRID:AB_2881191
Anti GSTP1 mAb	Cell Signaling Technology	Cat#CST3369; RRID:AB_2279558
Anti-phospho-SAPK/JNK m/Ab	Cell Signaling Technology	Cat#CST4668T; RRID:AB_823588
Anti-JNK mAb	ABclonal	Cat#A4867; RRID:AB_2863367
Anti-β-tubulin mouse monoclonal antibody	Abbkine	Cat#ABL1030
Biological samples		
Human cervical cancer tumors	Tongji Hospital, Tongji Medical College	TJ-IRB20180505
Chemicals, peptides, and recombinant proteins		
NBDHEX	MedChemExpress	Cat#HY-135318
Cisplatin	MedChemExpress	Cat#HY-17394
CY3	Servicebio	Cat#GB21303
WesternBright ECL HRP Substrate	Advansta	Cat#K-12045-D50
FITC	Servicebio	Cat#GB21301
TRIzol	Invitrogen	Cat#15596026
Matrigel	BD Biosciences	Cat#356234
Critical commercial assays		
CCK8	Vazyme	Cat#A311
Annexin V-FITC/PI kit	BD Biosciences	Cat#556547
Cell Total RNA Isolation Kit	Vazyme	Cat#RC112
ChamQ Universal SYBR qPCR Master Mix	Vazyme	Cat#Q711
GST activity assay kit	Solarbio Life Science	Cat#BC0355
Bradford protein assay kit	Servicebio	Cat#G2001
Reverse Transcription Kit	Vazyme	Cat#R323
Deposited data		
Raw and processed RNA-seq data	This paper	GSE235366, GSE235466
Experimental models: Cell lines		
Human ceivical cancer cells: SiHa	ATCC	Cat#HTB-35
Human ceivical cancer cells: ME180	Procell	Cat#CL-0155
Experimental models: Organisms/strains		
Mouse: BALB/cNj-Foxn1nu/Gpt	Gempharmatech	Cat#D000521
Oligonucleotides		
qPCR primer for VPS13C Forward/Reverse: CCCCAACAACAGACCCTGAA/ CCTCCGGAACCCAAAGACAA	This paper	N/A
qPCR primer for GSTP1 Forward/Reverse: CATCTACACCAACTATGAGGCG/ AGCAGGGTCTCAAAAGGCTTC	This paper	N/A
qPCR primer for β-Actin Forward/Reverse: CATGTACGTTGCTATCCAGGC/ CTCCTTAATGTCACGCACGAT	This paper	N/A

(*Continued on next page*)

Continued

REAGENT or RESOURCE	SOURCE	IDENTIFIER
shVPS13C-1 RNA sequence: CGGACAAAGTTAATCCAACAA	This paper	N/A
shVPS13C-2 RNA sequence: GCAAAGGTCAATAGGCTTATA	This paper	N/A
shVPS13C-3 RNA sequence: GCAGTAACTAATGCCCTAAAT	This paper	N/A
sgVPS13C-1 RNA sequence: GACTTGCTGAACCGCTTCCT	This paper	N/A
sgVPS13C-2 RNA sequence: AGAAGCAGTTGTTGCGACCC	This paper	N/A
Recombinant DNA		
psi-LVRU6GP LentiCRISPR v2	Addgene	Cat#52961
lenti-CRISPRa	Addgene	Cat#75112
pMDLg/pRRE	Addgene	Cat#12251
pRSV-Rev	Addgene	Cat#12253
pCMV-VSV-G	Addgene	Cat#8454
Software and algorithms		
ImageJ	Schneider	RRID: SCR_003070
FlowJo v10	https://www.flowjo.com/	RRID: SCR_008520
GraphPad Prism 7.0	http://www.graphpad.com/	RRID: SCR_002798
Kaplan–Meier plotter	http://kmplot.com/	RRID: SCR_018753
TIDE web tool	https://tide.nki.nl/	N/A
Genomics of Drug Sensitivity in Cancer (GDSC) database	https://www.cancerrxgene.org/	N/A
LinkedOmics database	http://www.linkedomics.org/	N/A

RESOURCE AVAILABILITY

Lead contact

Further information and requests for resources and reagents should be directed to and will be fulfilled by the Xun Tian (tianxun@zxhospital.com).

Materials availability

This study did not generate new unique reagents.

Data and code availability

RNA-sequencing data generated in the present study have been submitted to GEO database and are publicly available. The accession number is listed in the key resources table. This paper does not report original code. Any additional information required to reanalyze the data reported in this paper is available from the lead contact upon request.

EXPERIMENTAL MODEL AND SUBJECT DETAILS

Cell lines

The cervical cancer cell line SiHa was purchased from the American Type Culture Collection (ATCC) and cultured in Dulbecco's modified Eagle's medium (DMEM). The human cervical epidermoid carcinoma cell line ME180 was purchased from Procell Life Science & Technology (Wuhan, Hubei, China). DMEM and McCoy's 5A medium were supplemented with 10% fetal bovine serum (FBS, Gibco) and 100 U/ml penicillin and streptomycin (Invitrogen). The cell incubator was set in humidified air with 5% CO2 at 37°C and sterilized regularly. Cisplatin-resistant SiHa cells (SiHa/DDP) were developed by exposure to continuously increasing concentrations of cisplatin from the parental SiHa cells. The viability of SiHa and SiHa/DDP cells

was confirmed by the CCK-8 assay. The cell lines used in the study were authenticated from a national cell repository facility by short tandem repeats (STR) profiling and were tested for mycoplasma contamination on a regular basis.

Tumor xenograft studies

SiHa cells (5×10^6) with or without VPS13C knockdown were injected with Matrigel (BD Biosciences) into the flanks of 4- to 6-week-old female nude mice. These mice were grouped into four groups, with six mice in each group. Once the tumor volume reached 80–100 mm^3 two weeks later, cisplatin (2 mg/kg or 5 mg/kg) and NBDHEX (6 mg/kg) were administered by intraperitoneal (i.p.) injection every three days and by mouth every day, respectively. Tumor volume was measured every 2 days and was calculated by the following formula: (long diameter) × (short diameter)^2/2. Three weeks later, the mice were sacrificed, and the tumors were harvested and analyzed. Animal experiments were approved by the institutional committee at Wuhan Servicebio Technology Co., Ltd. The ethical approval protocol number was Servicebio Animal Welfare NO.2022145.

Tumor samples

Tumor samples from cervical cancer patients were collected from Tongji Hospital, Tongji Medical College, Huazhong University of Science and Technology. This research was approved by the Ethical Committee of Tongji Hospital, Tongji Medical College, Huazhong University of Science and Technology (approval number: TJ-IRB20180505).

METHOD DETAILS

Plasmid construction

Short hairpin RNA (shRNA) was used to establish stable VPS13C-knockdown SiHa cells and the clustered regularly interspaced short palindromic repeats (CRISPR)/Cas9 system was used to generate VPS13C-knockout ME180 cells. For the CRISPR/Cas9 procedure, single guide RNAs (sgRNAs) targeting the VPS13C gene were designed using online tools (http://crispr.tefor.net/). All of the sequences were synthesized and purified by Sangon Biotech (Shanghai, China) and cloned into Lentiviral psi-LVRU6GP LentiCRISPR v2 (Addgene plasmid, #52961). The CRISPR activation (CRISPRa) system was used for VPS13C overexpression in SiHa and ME180 cells.[43,44] gRNA targeting the VPS13C transcription start site region was designed to construct overexpression plasmids. Negative control gRNAs that do not exist in the human genome were retrieved from Addgene (#75112).

Lentivirus production and transduction

HEK293T cells were seeded in a 10 cm cell culture dish before transfection. Then, 4.2 μg of pMDLg/pRRE, 2.1 μg of pRSV-Rev, 3.1 μg of pCMV-VSVG, and 4.1 μg of lentiviral psi-LVRU6GP were cotransfected with polyethyleneimine (PEI). After 72 h, the virus-containing medium was collected and filtered through a 0.45-μm sterilizing filter. Then, it was mixed with an equal volume of serum-free DMEM to transduce overnight SiHa and ME180 cells at 30–50% confluence. After 12 h, the medium was refreshed with DMEM containing 10% FBS and incubated for 72 h. Stable VPS13C low-expression and puromycin-resistant SiHa and ME180 cells were selected by 1 μg/mL puromycin for 72 h.

Tracking of indels by decomposition (TIDE)

Tracking of Indels by Decomposition (TIDE)[45] can accurately identify and quantify insertions and deletions that arise after the introduction of double-strand breaks (DSBs). It involves three simple steps, one pair of standard PCRs, one pair of the standard capillary ("Sanger") sequencing reactions, and an analysis of the two resulting raw sequencing files using the TIDE web tool (http://shinyapps.datacurators.nl/tide/).

Cell viability assays

The viability of the cells was evaluated by a CCK-8 assay according to the manufacturer's instructions. Briefly, the cells were seeded into 96-well plates in triplicate and cultured overnight. After 24 h, cells were treated with different concentrations of cisplatin. After 48 h of incubation, CCK-8 (10 μL) was added to each well and further incubated at 37°C for 2 h before detection. The optical density values were measured at 450 nm using a microplate reader. The combination index (CI) was calculated using CompuSyn software with the Chou-Talalay equation,[46] which allows the identification of an additive effect (CI = 1), synergistic effect (CI < 1), or antagonistic effect (CI > 1) in drug combinations.

Analysis of apoptosis by flow cytometry

SiHa or ME180 cells were treated with 20 μM and 2 μM cisplatin for 48 h with or without NBDHEX. Cell apoptosis was examined according to the manufacturer's instructions for the Annexin V-FITC/PI kit (BD Biosciences Pharmingen, San Jose, CA). Cells were detached with 0.25% EDTA-free trypsin, washed twice with cold PBS, and then resuspended in binding buffer at a concentration of 1×10^6 cells/ml. Afterward, each sample was sustained with 5 μL of FITC Annexin V and 5 μL PI and incubated for 15 min at room temperature (25°C) in the dark. Then, 400 μL of 1× binding buffer was added to each tube and analyzed by flow cytometry within 1 h.

RNA extraction and qPCR assays

The total RNA of the cultured cells was extracted and purified by the Cell Total RNA Isolation Kit (Vazyme, RC112). The extracted RNA was reverse transcribed into cDNA using a Reverse Transcription Kit (Vazyme, R323). Real-time quantitative PCR (qPCR) was performed using ChamQ Universal SYBR qPCR Master Mix (Vazyme, Q711). The total reaction system was 20 μL, including 0.5 μL cDNA obtained from reverse transcription of 1 μg RNA, 0.4 μL of forward and reverse primers (10 μM), 10 μL of 2 × ChamQ Universal SYBR qPCR Master Mix, and variable ddH_2O to generate a volume of 20 μL. The samples underwent two-step amplification with an initial step at 95°C (30 s), followed by 95°C (10 s) and 60°C (30 s) for 40 cycles. Fold changes in the expression of each gene were calculated by the relative quantitative method ($2^{-\triangle\triangle CT}$ method).

Western blotting

Total protein was extracted from cells using RIPA lysis buffer (G2002, Servicebio Technology Co., Ltd., Wuhan, China) with 1x cocktail (G2006, Servicebio), 1% PMSF (Sigma, P8340), 1% NaF (G2007-1, Servicebio), and 1% NaVO3 (G2007-2, Servicebio). Protein concentration was determined by a Bradford protein assay kit (G2001, Servicebio). Protein lysates (20–30 μg per sample) were separated on 8 or 12% SDS-polyacrylamide gels, transferred to PVDF membranes (G6015, Servicebio), and incubated with primary and secondary antibodies, and the signal was detected following the commercial protocol using WesternBright ECL HRP Substrate (K-12045-D50, Advansta). Anti-β-tubulin mouse monoclonal antibody (ABL1030) was purchased from Abbkine. GSTP1 (CST3369) and phospho-SAPK/JNK (Thr183/Tyr185) (CST 4668T) antibodies were purchased from Cell Signaling Technology. Antibodies against JNK (A4867) and VPS13C (28676-1-AP) were purchased from ABclonal and Proteintech, respectively. HRP-labeled secondary antibodies (GB23301, GB23303) were purchased from Servicebio Technology Co., Ltd., Wuhan, China.

Immunofluorescence analysis

Cells were seeded on coverslips and fixed with 4% paraformaldehyde in PBS for 15 min at room temperature. The cells were then permeabilized with 0.1% Triton X-100 in PBS for 10 min at 4°C and blocked with 1% bovine serum albumin (BSA; Servicebio, G5001) in PBS for 30 min. Then, the cells were incubated with the indicated primary antibodies overnight at 4°C or room temperature for 1 h. After washing with PBS containing 0.1% Tween 20, the cells or sections were incubated with CY3 (GB21303, Servicebio) and FITC (GB21301, Servicebio) for 2 h. The cells were then washed and counterstained with DAPI for 5 min and mounted with antifade reagent. Slides were viewed and photographed with a Leica microscope, and the images were processed in Photoshop (Adobe Systems).

Immunohistochemistry

The expression of VPS13C in cervical cancer tissue was detected by immunohistochemistry. The slices of the relevant arrays were baked at 60°C for 2 h, deparaffinized twice in xylene for 15 min, and dehydrated with an alcohol gradient. Antigen retrieval was conducted by boiling for 10 min in 0.01 M citric acid buffer and blocking in goat serum for 60 min at room temperature. The slices were incubated with primary anti-VPS13C antibody (28676-1-AP, Proteintech, USA) diluted 1:100 overnight at 4°C, incubated with secondary antibody, and rinsed with PBS. The antibody complex was detected with avidin-biotin-peroxidase complex solution and stained with 3,3′-diaminobenzidine (DAB). PBS was used as a negative control instead of primary antibody.

GST activity assays

After 48 h of exposure to cisplatin, control/VPS13C-silenced cells were detected for GST enzyme activity using a commercial GST activity assay kit (BC0355, Solarbio Life Science, Beijing, China). Briefly, 1 volume

(mL) of the reagent was added to the cells at a ratio of 500~1000:1 (it is recommended to add 1 mL of reagent to 1 to 5 million cells), and the cells were sonicated in an ice bath (power 300 W, ultrasonic for 3 s, interval 7 s, total time 3 min). Then, the sample was centrifuged at 8000 × g for 10 min at 4°C, and the supernatant was placed on ice for testing. We defined activity units by protein concentration calculations: At 25°C or 37°C, 1 μmol of CDNB combined with GSH was catalyzed as one unit of enzyme activity per milligram of protein per minute. GST (U/mg prot) = [(A4-A3) - (A2-A1)] ÷ (ε×d) × 106 × V inverse total ÷ (Cpr × V sample) ÷ T = 0.38 × [(A4-A3) - (A2-A1)] ÷ Cpr.

Kaplan–Meier plotter analysis

Kaplan–Meier plotter (http://kmplot.com/) is capable of assessing the effect of 54 k genes (mRNA, miRNA, protein) on survival in 21 cancer types from databases including GEO, EGA, and TCGA.[47] Survival curves were evaluated using Kaplan–Meier. We used Kaplan–Meier plotter to assess the prognostic value of VPS13C mRNA in patients with lung cancer, breast cancer, and gastric cancer. The hazard ratio (HR) with 95% confidence interval and log rank p values were calculated and shown.

LinkedOmics analysis

The LinkedOmics database (http://www.linkedomics.org/login.php) is a publicly available portal that includes multiomics data from all 32 TCGA cancer types and 10 Clinical Proteomics Tumor Analysis Consortium (CPTAC) cancer cohorts.[48] The LinkedOmics database was used to investigate the transcription networks of GSTP1 and VPS13C in cervical cancer. In addition, we used the "Linked Interpreter" module to conduct a biological analysis of VPS13C and related overlapping genes by GSEA; this analysis revealed enriched biological processes and Kyoto Encyclopedia of Genes and Genomes (KEGG) pathways. The rank criterion was a false discovery rate (FDR) < 0.05, the minimum number of genes was 3, and the number of simulations was 1000.

GDSC database

The chemosensitivity of tumors is mainly analyzed using the Genomics of Drug Sensitivity in Cancer (GDSC) database, which is currently the largest public resource library for drug sensitivity and related markers of cancer cells.[49] It contains data on the response of more than 1000 tumor cells to different anticancer drugs (available at https://www.cancerrxgene.org/).

RNA sequencing and analysis

Total RNA was extracted from the tissues using TRIzol (Invitrogen, Carlsbad, CA, USA) according to the manufacturer's instructions. Subsequently, total RNA was qualified and quantified using a NanoDrop and Agilent 2100 bioanalyzer (Thermo Fisher Scientific, MA, USA). The final library was amplified with phi29 to make DNA nanoballs (DNBs), which had more than 300 copies of one molecule. DNBs were loaded into the patterned nanoarray, and single-end 50-base reads were generated on the DNBSEQ platform (BGI-Shenzhen, China). mRNA-sequencing analysis was performed by Huada Genomics Institute (BGI). KEGG pathway analysis and gene set enrichment analysis (GSEA) were conducted with the Dr. Tom program (https://biosys.bgi.com).

QUANTIFICATION AND STATISTICAL ANALYSIS

Statistical analyses were performed using the GraphPad Prism 7.0 package (GraphPad Software, Inc., La Jolla, CA, USA). Error bars represent the mean ± standard deviation (SD) or mean ± standard error of the mean (SEM). Independently performed biological replicates are indicated as dots in the bar graphs, and all biological replicates were more than or equal to 3 ($n \geq 3$). Statistical methods for each analysis are described in figure legends. In all analyses, the significance level is presented as follows: *$p < 0.05$, **$p < 0.01$, ***$p < 0.001$, ****$p < 0.0001$, $^{\#}p < 0.05$, $^{\#\#}p < 0.01$, $^{\#\#\#}p < 0.001$, $^{\#\#\#\#}p < 0.0001$, ns represents "not significant".